

## Green Synthesis, Characterization and Antimicrobial Activity of Zinc Oxide Nanoparticles on Clinical Isolates of *Streptococcus pyogenes*

S. AKASH, N. AHALYA and P. DHAMODHAR\*

Department of Biotechnology, M.S. Ramaiah Institute of Technology, Bangalore-560054, India

\*Corresponding author: Fax:+91 80 23603124; Tel: +91 80 2360 3122; E-mail: dhamu\_bio@msrit.edu; dhamu.bio@gmail.com

Received: 14 October 2019;

Accepted: 7 December 2019;

Published online: 25 February 2020;

AJC-19811

Zinc oxide nanoparticles were synthesized using epicarp of *Punica granatum* by combustion method at moderate temperatures. Zinc oxide nanoparticles obtained in agglomerate form were characterized by powder X-ray diffractometer (PXRD) and found to have hexagonal phase, wurtzite structure. The crystalline size of nanoparticle was found to be ~ 60 nm by using Debye-Scherrer formula. The morphology Index, Lorentz factor and Lorentz polarization factor were also calculated. Ultraviolet-visible spectroscopy (UV-vis) spectrum for ZnO nanoparticle showed a strong absorbance at 374 nm. This corresponds to the calculated band gap energy of 3.48 eV and the particle size calculated using band gap was found to be 50 nm. The Fourier Transform Infrared Spectroscopy (FTIR) spectrum showed a peak at 499  $\text{cm}^{-1}$ , which indicated Zn-O stretch bond. The scanning electron microscopy (SEM) analysis proved the size of nanoparticles synthesized were around 50 nm and energy dispersive X-ray spectroscopy (EDS) revealed the elemental composition of zinc oxide nanoparticles. The ZnO-NPs were evaluated for antibacterial activity against gram positive, tonsillitis causing *Streptococcus pyogenes*. From the present study, it was concluded that zinc oxide nanoparticles synthesized by combustion method could be valuable and economic in the field of nanotechnology.

**Keywords:** Zinc oxide nanoparticles, Combustion, *Punica granatum*, Antibacterial activity.

### INTRODUCTION

Zinc Oxide nanoparticles are gaining importance for its unique physical and chemical properties, ability to have high chemical stability, high electrochemical coupling coefficient, broad range of radiation absorption and high photo-stability [1,2]. The structures of ZnO nanoparticles determine their applications in the field of nanotechnology. Zinc oxide material with various shapes, such as, nano-tubes, nano-ribbons, nano-wires, nano-belts, tripods, spherical nanoparticles, hollow spheres, nano-needles, mushrooms, hexagonal columns, snow-flakes and so on, have aroused much interest [3]. ZnO provides one of the greatest assortments of varied particle structures among all known materials. ZnO nanoparticles are usually synthesized by thermal decomposition, thermolysis, chemical vapor deposition, sol-gel, spray pyrolysis, precipitation, vapour phase oxidation, thermal vapor transport, condensation and hydrothermal methods [4]. These approaches use physical and chemical methods involving complex procedures, sophisticated equipment and rigorous experimental conditions. Hence,

there is a need to find economically viable synthesis techniques. The synthesis of nanoparticles by combustion method is emerging as a promising technique for the preparation of nanopowders. This process is simple, fast and economic and does not require high-temperature furnaces and complicated set-ups [5].

Green syntheses of nanoparticles from plants are more stable, varied shape and size and limits the exposure, utilization of toxic and expensive chemicals [6]. The choice of fuel significantly impacts the exothermicity and the amount of gases that evolve during combustion process. This in turn has a strong influence on properties of the product [7]. The fuels employed regularly in the combustion synthesis are glycine, citric acid, urea, oxalyl dihydrazide and carbonyl dihydrazide [8]. Complexing ability is one of the primary characteristics that a fuel should possess. Among the complexing agents, *Punica granatum* is known to be particularly efficient due to the presence of amine atoms as functional groups in their molecules [9].

Group A *Streptococcus* (GAS), a human pathogen is responsible for a number of suppurative human infections. It can cause

many diseases ranging from mild impetigo, pharyngitis, scarlet fever to more severe and serious toxic shock syndrome and suppurative sequelae such as glomerulonephritis. *Streptococcus pyogenes*, often referred to as Group A *Streptococcus* bacteria, can cause impetigo, scarlet fever, puerperal fever, streptococcal toxic shock syndrome, strep throat, tonsillitis and other upper respiratory tract infections. Necrotizing fasciitis, a rapidly spreading infection of the skin and underlying tissue caused by *S. pyogenes*, has been popularly referred to as flesh-eating disease [10,11].

Penicillin and its derivatives remain the drugs of choice for streptococcal infections as GAS remains uniformly susceptible to them. However, due to the reported high rates of clinical failure and penicillin hypersensitivity in patients allergic to penicillin, alternative antibiotics such as macrolides and quinolones are prescribed. However increasing incidence of resistance to antibiotics is reported worldwide [11,12]. As a consequence, individuals who suffer group A streptococcal pharyngeal infections may develop acute rheumatic fever and rheumatic heart disease, which is a major problem in developing countries like India [13]. Severe GAS-associated disease is estimated to be 18.1 million cases worldwide [14].

In the present study, synthesis of spherical shaped nano crystalline ZnO powders by combustion method using *Punica granatum* is reported. The combustion reaction is initiated in a muffle furnace at  $400 \pm 10$  °C [3]. The synthesized nano powders were characterized for their structure using powder X-ray diffraction (PXRD). The morphological studies were also carried out using scanning electron microscopy (SEM). Fourier transformed infrared (FTIR) and UV-visible spectroscopy were employed to investigate synthesized nano-powders. Finally, ZnO nanoparticles were tested against the clinical isolates of group A streptococcus.

## EXPERIMENTAL

**Preparation of plant extract:** Fresh native varieties of *Punica granatum* were purchased from Safal market, Bangalore, India. The epicarp of *Punica granatum* was separated from mesocarp, endocarp and seeds. Then separated *Punica granatum* epicarp was made into a fine paste and mixed with 50 mL of deionized water. The diluted *Punica granatum* epicarp solution was used for the synthesis of zinc oxide nanoparticle by combustion method.

**Synthesis of nanoparticles:** Zinc nitrate (1 M) was prepared using deionized water and then added *Punica granatum* epicarp solution. The continuous stirring of materials was carried out for homogeneity in mixing of contents. The mixture of zinc nitrate and *Punica granatum* epicarp solution was kept in a muffle furnace at 400 °C for 30 min. After cooling for about 0.5 h, zinc oxide nanoparticles were scrapped out and stored for further applications.

**Characterization of green synthesized nanoparticles:** The phase purity and crystalline nature of green synthesized zinc oxide samples were examined by powder X-ray diffractometer (Bruker-D2-Phaser) using  $\text{Cu K}\alpha$  (1.541 Å) radiation with a nickel filter. Scanning electron microscopy along with energy dispersive X-ray spectroscopy (EDS) (Zeiss Gemini-Ultra 55) was used to examine the morphology on surface of nano-

particles. The SEM micrograph was recorded after vacuum dissection of ZnO nanoparticles and coating the samples with gold. The Bruker-Alpha FT-IR spectrometer with KBr pellets were used for FTIR studies. The UV-visible absorption spectrum of nanoparticles was recorded.

**Isolation of *Streptococcus pyogenes*:** About 20 pediatric cases of the age group 5 to 15 years suspected for pharyngotonsillitis infection and receiving no antibiotics in antecedent for 7 days visiting M.S. Ramaiah hospital, Bengaluru, India were subjected to repeat throat samplings. Standard *Streptococcus pyogenes* strain MTCC 442 received from Microbial Type Culture Collection and Gene Bank, Institute of Microbial Technology, Chandigarh, India and ATCC 19615 received from M.S. Ramaiah Metropolis hospital were also included as control.

**Antibacterial susceptibility:** All the isolates identified as group A *Streptococcus* were tested for their sensitivity pattern with the green synthesized ZnO nanoparticles by agar well diffusion method on Mueller-Hinton agar (MHA) as recommended by the Clinical and Laboratory Standards Institute, Wayne, USA. The anti-GAS activity at various concentrations (10, 20, 30 and 40 mg/mL) and dilutions of synthesized ZnO nanoparticles was screened by well diffusion technique on sterile Muller Hinton agar plates. Antibacterial activity in terms of zone of inhibition (mm) was recorded after 24 h of incubation.

## RESULTS AND DISCUSSION

Zinc Oxide nanoparticles were synthesized by combustion method using *Punica granatum* epicarp. The obtained zinc oxide nanoparticles were yellowish white in colour. The diluted *Punica granatum* epicarp solution was used as fuel and zinc nitrate served as an oxidizer for the synthesis of nanoparticles by combustion process. The time factor to synthesize these nanoparticles in this method was a major advantage. In combustion process the solution mixture started boiling initially and underwent dehydration. Subsequently, it decomposed with formation of huge amounts of oxides of carbon and nitrogen gases. It was accompanied by impulsive smoldering with huge swelling of the reaction mixture. This in turn produced foam-covered and capacious zinc oxide nanoparticles as powder.

**Powder XRD analysis:** Fig. 1 and Table-1 shows the PXRD pattern for zinc oxide particles synthesized by combustion method using *Punica granatum* epicarp as fuel. Zinc oxide powder were studied at diffraction angles from 20°-80°. All diffraction peaks corresponding to (1 0 0), (0 0 2), (1 0 1), (1 0 2), (1 1 0), (1 0 3), (1 1 2) planes were in agreement with typical hexagonal wurtzite structure of pure ZnO belonging to JCPDF no. 36-1451 [3]. The phase purity of the sample was confirmed with no additional peaks corresponding to any secondary or impurity phase. Debye-Scherrer formula was used to calculate the diameter of green synthesized ZnO nanoparticles. The ZnO nanoparticles showed an average crystalline size of about 63.87 nm corresponding to the plane 101 located at 35.86°.

**UV-visible analysis:** The green synthesized ZnO nanoparticles were further characterized using UV-visible spectroscopy, which showed a typical absorption at 374 nm (Fig. 2). The spectrum also indicated that nanomaterial synthesized in the present study was pure, as the spectrum showed a smooth line, beyond the original drop. If the sample had any contami-

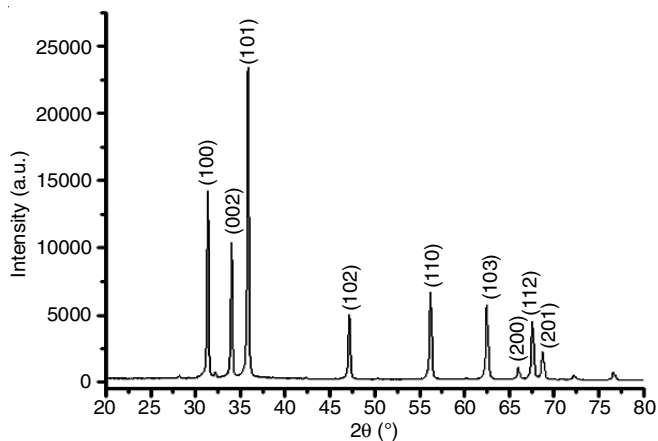


Fig. 1. PXRD pattern for ZnO nanoparticles synthesized by combustion method

2θ	h k l	Morphology index	Lorentz factor	Lorentz polarization factor
31.3758	1 0 0	0.6359	3.5516	24.5621
34.0361	0 0 2	0.6231	3.0523	20.5923
35.8649	1 0 1	0.6174	2.7718	18.3675
47.1655	1 0 2	0.5774	1.7043	9.9676
56.2335	1 1 0	0.5441	1.3168	6.6823
62.5158	1 0 3	0.5198	1.0862	5.2692
67.6135	1 1 2	0.5	0.9719	4.4519

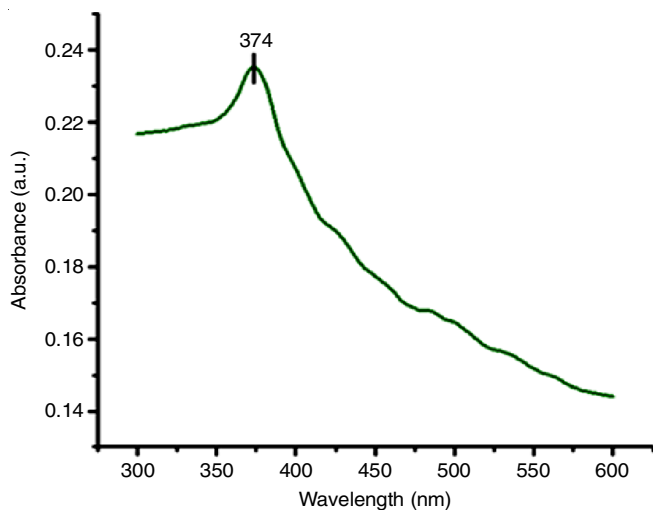


Fig. 2. UV-visible pattern for green synthesized ZnO nanoparticles

nants, they would have acted as dopants in the semiconductor material, causing lower energy (higher wavelength) transitions. This would be reflected as small peaks or drops above the original drop of the band gap. UV-Vis measurements can also be used to evaluate the functionalization of nanoparticles.

It was evident that significant sharp absorption of ZnO indicated the monodispersed nature of the nanoparticles [15]. From the effective mass model, a diameter of the particle size was calculated and was found to have an average size of 50 nm, which is similar to the size found through SEM.

**FTIR analysis:** The FTIR spectra of ZnO nanoparticles synthesized by combustion method is shown in Fig.3. A weak

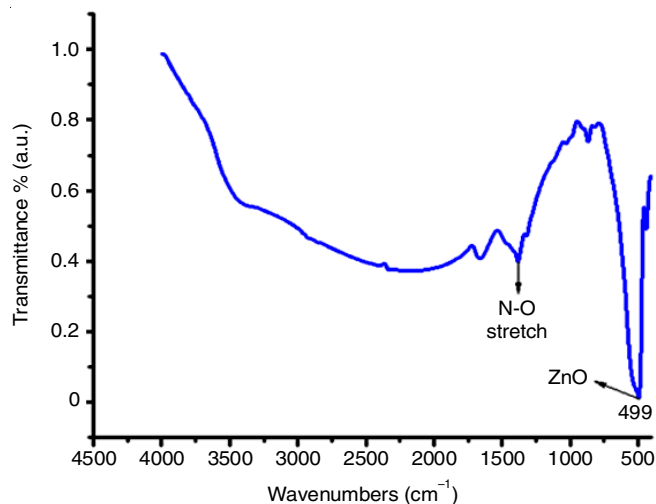


Fig. 3. FTIR spectrum for ZnO nanoparticles synthesized by combustion method

band at  $3500\text{ cm}^{-1}$  was attributed to the characteristic stretching mode of  $\text{H}_2\text{O}$  [16]. Small peaks at around  $2300\text{ cm}^{-1}$  showed the presence of (-CN) nitrite group [17]. The sharp peaks near  $1600\text{ cm}^{-1}$  indicated the trace amount of nitrates [18]. These bands confirm the presence of impurities in the sample, which is due to the incomplete combustion in fuel-lean synthesis runs. Bands ranging from  $600\text{--}400\text{ cm}^{-1}$  originate from metal to oxygen (M-O) groups. The band at  $499\text{ cm}^{-1}$  corresponds to stretching frequency of Zn-O hexagonal phase [3].

**SEM analysis:** The morphology of the synthesized nanoparticles showed the formation of agglomerated ZnO nanoparticles having wurtzite structure. The SEM analysis confirmed the approximated form of nanoparticles and most of the particles exhibited some faceting. It was observed that size of the nanoparticles were less than 100 nm (Fig. 4). It is evident that zinc oxide nanoparticle were in the range mentioned in literature [3]. The two vital uniqueness of wurtzite configuration are the non-central symmetry and polar surfaces. The structure of ZnO can be explained as a number of alternating planes poised of tetrahedrally coordinated  $\text{O}^{2-}$  and  $\text{Zn}^{2+}$  ions, stacked alternately along the  $c$ -axis. The oppositely charged ions produce positively charged zinc and negatively charged oxygen polar surfaces, resulting in a normal dipole moment and spontaneous polarization along the  $c$ -axis, as well as a divergence in surface energy leads to a wurtzite as the polymorphic modifications [19]. The impurities of *Punica granatum* epicarp were also found. In wurtzite, there are only ionic bonds. Hexagonal rings in the chair form with alternate positions occupied by  $\text{Zn}^{2+}$  and  $\text{O}^{2-}$  ions can be easily found in the structure.

**EDS analysis:** The EDS of ZnO sample carried out along with SEM revealed that the required composition of ZnO were present. Elemental composition of zinc was found to be 51.78 % and oxygen was 48.22 % (Fig. 5). This is in agreement with the ZnO nanoparticle, which is in 1:1 ratio. The slight variation in the composition is due to the loss of X-rays being detected [8]. The peak located on the left part of spectrum at 0.5 keV was clearly indicated the oxygen characteristic line, which confirms the presence of stabilizers.

**Agar well diffusion analysis:** Fig. 6 shows a line plot of isolate (no.) versus zone of inhibition (mm) of group A strepto-

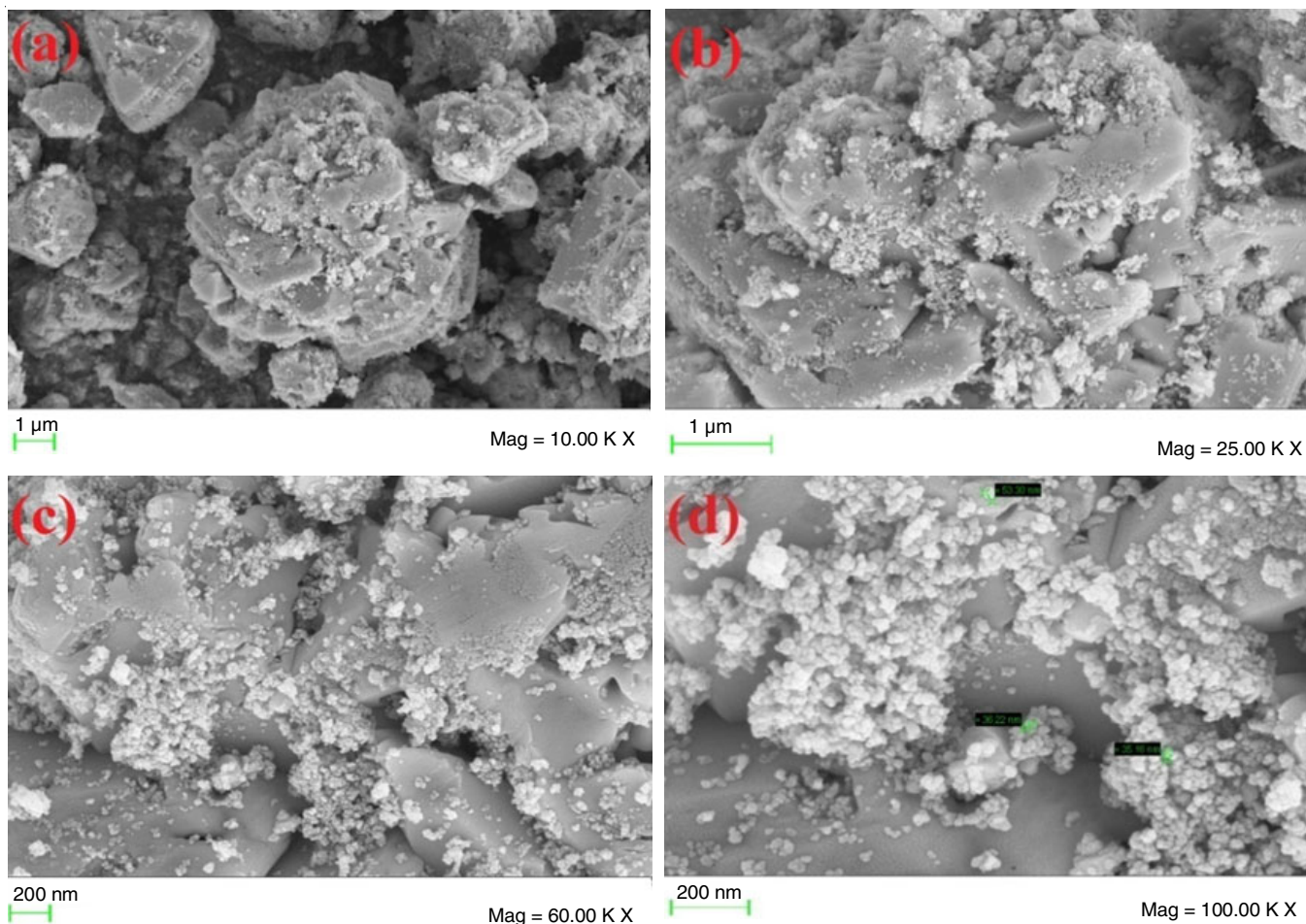


Fig. 4. SEM image of green synthesized ZnO nanoparticles

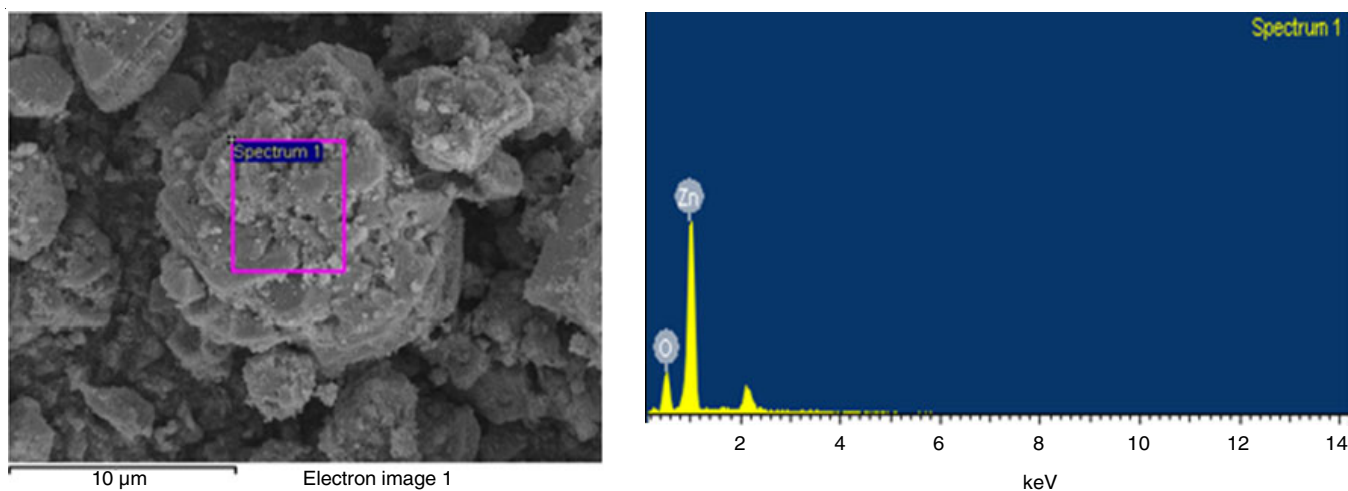


Fig. 5. EDS images showing elemental composition of ZnO nanoparticles

*coccus*. Out of the 20 clinical isolates obtained, only 8 isolates were tested positive for group A *streptococcus* and subjected for antibacterial studies. Standard isolate **s1** and **s2** exhibited a zone size of 18 mm and 19.5 mm, respectively, while the clinical isolates **s3**, **s4**, **s5**, **s6**, **s7** and **s8** exhibited zone of inhibition of 18, 22.5, 22.8, 19.9, 17.1 and 15.8 mm, respectively. The presence of inhibition zone clearly indicates that the mechanism of the biocidal action of ZnO nanoparticles, which involves disruption of the membrane with high rate of

generation of surface oxygen species and finally lead to the death of bacteria. Interestingly, size of the inhibition zone was different according to the type of isolates, where a similar work has been reported [20]. ZnO powder has been used for a long time as an active ingredient for dermatological applications in creams, lotions and ointments on account of its antibacterial properties. However, nanoparticles of ZnO are much more effective agents in controlling the growth of various microorganisms. The studies suggested that synthesized ZnO nanoparticles

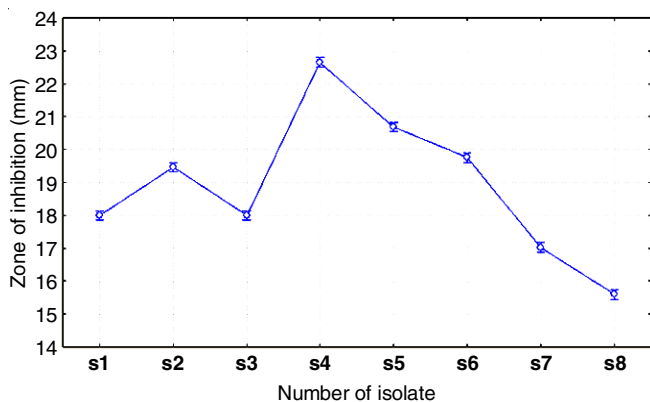


Fig. 6. Zone of inhibition versus clinical isolates of group A *Streptococcus*

are able to slow down the bacterial growth as a result of disorganization of *S. pyogenes* membranes, which increases the membrane permeability leading to the accumulation of nanoparticles in the bacterial membrane and cytoplasm regions of the cells [21,22]. The present research revealed that isolate s4 exhibited the maximum zone size, while isolate s8 exhibited the least. Overall results indicated that ZnO nanoparticles were effective in preventing the growth of group A streptococcus.

### Conclusion

Zinc oxide nanoparticles were synthesized by combustion method using *Punica granatum* epicarp as fuel. Powder X-ray diffraction patterns confirmed the hexagonal phase and the average crystallite size was found to be in the range of ~ 60 nm, which was in agreement with the SEM results. A transition of ZnO nanoparticles appeared at 374 nm and electronic band gap of ZnO formed was estimated to be 3.48 eV. SEM analysis showed that ZnO nanoparticles are in agglomerated form and characteristic impurities of *Punica granatum* were also observed. Zinc oxide nanoparticles synthesized using *Punica granatum* provides a way to use natural resources without involving chemical methods. The ZnO nanoparticles were further tested for their antibacterial activity on clinical isolates of group A *Streptococcus* and found effectively in preventing the growth of group A *Streptococcus*.

### CONFLICT OF INTEREST

The authors declare that there is no conflict of interests regarding the publication of this article.

### REFERENCES

- M. Roberson, V. Rangari, S. Jeelani, T. Samuel and C. Yates, *Nano Life*, **4**, 1440003 (2014); <https://doi.org/10.1142/S1793984414400030>
- S. Triboulet, C. Aude Garcia, L. Armand, A. Gerdil, H. Diemer, F. Proamer, V. Collin-Faure, A. Habert, J.-M. Strub, D. Hanau, N. Herlin, M. Carrière, A. Van Dorselaer and T. Rabilloud, *Nanoscale*, **6**, 6102 (2014); <https://doi.org/10.1039/C4NR00319E>
- A.J. Reddy, M.K. Kokila, H. Nagabhushana, J.L. Rao, C. Shivakumara, B.M. Nagabhushana and R.P.S. Chakradhar, *Spectrochim. Acta A Mol. Spectrosc.*, **81**, 53 (2011); <https://doi.org/10.1016/j.saa.2011.05.043>
- A. Kolodziejczak-Radzimska and T. Jesionowski, *Materials*, **7**, 2833 (2014); <https://doi.org/10.3390/ma7042833>
- A. Varma, A.S. Mukasyan, A.S. Rogachev and K.V. Manukyan, *Chem. Rev.*, **116**, 14493 (2016); <https://doi.org/10.1021/acs.chemrev.6b00279>
- A. Umamaheswari, S. Lakshmana Prabu and A. Puratchikody, *MOJ Bioequiv. Availab.*, **5**, 151 (2018); <https://doi.org/10.15406/mojbb.2018.05.00096>
- M.A. Aghayan and M.A. Rodriguez, *Mater. Sci. Eng.*, **32**, 2464 (2012); <https://doi.org/10.1016/j.msec.2012.07.027>
- R.H. Krishna, B.M. Nagabhushana, H. Nagabhushana, R.P.S. Chakradhar, R. Sivaramakrishna, C. Shivakumara and T. Thomas, *J. Alloys Compd.*, **585**, 129 (2014); <https://doi.org/10.1016/j.jallcom.2013.09.037>
- M. Goudarzi, N. Mir, M. Mousavi-Kamazani, S. Bagheri and M. Salavati-Niasari, *Sci. Rep.*, **6**, 32539 (2016); <https://doi.org/10.1038/srep32539>
- C. Plainvert, M. Dimis, M. Ravins, E. Hanski, G. Touak, N. Dmytruk, A. Fouet and C. Poyart, *J. Clin. Microbiol.*, **52**, 2003 (2014); <https://doi.org/10.1128/JCM.00290-14>
- T. Abraham and S. Sistla, *Int. J. Med. Microbiol.*, **36**, 186 (2018); [https://doi.org/10.4103/ijmm.IJMM\\_18\\_107](https://doi.org/10.4103/ijmm.IJMM_18_107)
- B. Lu, Y. Fang, Y. Fan, X. Chen, J. Wang, J. Zeng, Y. Li, Z. Zhang, L. Huang, H. Li, D. Li, F. Zhu, Y. Cui and D. Wang, *Front. Microbiol.*, **8**, 1052 (2017); <https://doi.org/10.3389/fmicb.2017.01052>
- P.C. Negi, S. Sondhi, S. Asotra, K. Mahajan and A. Mehta, *Indian Heart J.*, **71**, 85 (2019); <https://doi.org/10.1016/j.ihj.2018.12.007>
- A. Ba-Saddik, A. Munibari, A.M. Alhilali, S.M. Ismail, F.M. Murshed, J.B.S. Coulter, L.E. Cuevas, C.A. Hart, B.J. Brabin and C.M. Parry, *Trop. Med. Int. Health*, **19**, 431 (2014); <https://doi.org/10.1111/tmi.12264>
- Y.T. Prabhu, K.V. Rao, V.S.S. Kumar and B.S. Kumari, *Adv. Nanopart.*, **2**, 45 (2013); <https://doi.org/10.4236/anp.2013.21009>
- D. Mishra, S. Anand, R.K. Panda and R.P. Das, *Mater. Chem. Phys.*, **86**, 132 (2004); <https://doi.org/10.1016/j.matchemphys.2004.02.017>
- AC. Tas, *J. Am. Ceram. Soc.*, **81**, 2853 (1998); <https://doi.org/10.1111/j.1151-2916.1998.tb02706.x>
- V. Singh, R.P.S. Chakradhar, J.L. Rao and H.Y. Kwak, *J. Lumin.*, **131**, 247 (2011); <https://doi.org/10.1016/j.jlumin.2010.10.006>
- A.P. Uthirakumar, ed.: L.A. Kosyachenko, Fabrication of ZnO Based Dye Sensitized Solar Cells, Intech Open, London, Chap. 19, p. 435 (2011).
- S. Gunalan, R. Sivaraj and V. Rajendran, *Progr. Nat. Sci. Mater. Int.*, **22**, 693 (2012); <https://doi.org/10.1016/j.pnsc.2012.11.015>
- K.S. Siddiqi, A. ur Rahman, Tajuddin and A. Husen, *Nanoscale Res. Lett.*, **13**, 141 (2018); <https://doi.org/10.1186/s11671-018-2532-3>
- N. Niño-Martínez, M.F. Salas Orozco, G.-A. Martínez-Castañón, F. Torres Méndez and F. Ruiz, *Int. J. Mol. Sci.*, **20**, 2808 (2019); <https://doi.org/10.3390/ijms20112808>